Sensor Alignment Calibration for Precision Attitude Determination of Spacecrafts

Il-Hyoung Lee*, Chang-Kyung Ryoo*, Hyochoong Bang, Min-Jea Tahk*** and Sang-Ryool Lee******
Division of Aerospace Engineering, KAIST
373-1 Guseong-dong Yuseong-gu Daejeon, Korea, 305-701

Abstract

A new alignment calibration method of attitude sensors for the precision attitude determination of a spacecraft based on the extended Kalman filter is proposed. The proposed method is divided into two steps connected in series: the gyro and the star tracker calibration. For gyro calibration, alignment errors and scale factor errors are estimated during the calibration maneuver under the assumption of a perfect star tracker. Estimation of the alignment errors of the star trackers and compensation of the gyro calibration errors are then performed using the measurements including payload information. Performance of the proposed method are demonstrated by numerical simulations.

Key Word : Attitude determination, Alignment, Calibration, Star tracker, Extended Kalman filter, Spacecraft

Introduction

Observation satellites with high resolution camera require arc-seconds attitude pointing accuracy. The pointing accuracy is basically dependent on the precision of attitude determination. It is known that such degree of precision is achieved by identifying and compensating the alignment errors of attitude sensor units [1-6]. Although the gyros are calibrated before the launch accurately enough to guarantee the required accuracy within a specified error budget, they can be misaligned by the impact due to rocket launch or thermal structural deformation of the base. Star trackers providing much higher accurate attitude information are used to isolate and compensate the misalignment of the gyros. However, the same alignment problems also occur in the star trackers. Recently, alignment Kalman filter(AKF) utilizing payload information to calibrate the absolute alignment of the star trackers has been presented[6]. Payload information obtained from the camera and ground control point (GCP) is as accurate as the star tracker when the spacecraft is not in maneuver. The structure of AKF is the same as the extended Kalman filter (EKF) [7] in which the bias, scale factor, and alignment errors of the gyros and star trackers are augmented as the filter states. This method shows good performance for the attitude determination and the sensor calibration, but it suffers from two problems in actual implementation. First, all the 21 states should be estimated[6] in the single filter structure so that it is hard to converge as well as hard to work in real time. Second, AKF requires a calibration maneuver to separate the alignment and scale factor errors from the bias of the gyros. During the

* Graduate student
E-mail : ihlee@fdcl.kaist.ac.kr, TEL : 042-869-3789, FAX : 042-869-5762
** Associate Professor
*** Professor
**** Researcher of Korea Aerospace Research Institute

calibration maneuver, it is expected that the performance of AKF will be significantly degraded, because the accuracy of payload information can be worsen by maneuver. Performance degradation of AKF during the calibration maneuver affects all the estimation result after the calibration maneuver.

Table 1. Alignment calibration

	Step 1	Step 2
States	Quaternion error(3) Bias error(3) Gyro scale factors(3) Gyro misalignments(6)	Quaternion error(3) Bias error(3) Star tracker misalignments(6)
Measurement devices	One star tracker Three rate gyros	Two star trackers Three rate gyros One payload information
Remark	Calibration maneuver	Gyro scale factors and misalignments update

In this paper, we propose an improved on-line attitude sensor calibration method for precision attitude determination in the practical implementation. The proposed alignment calibration procedure is divided into two steps as shown in Table 1. In step 1, identification of the alignment error from the gyro bias is conducted during the calibration maneuver. In the step 1, it is assumed that one of the star trackers is perfect. The estimated gyro scale factor errors and the alignment errors inevitably contain some errors due to the misalignment of the star trackers. Since the payload information during the calibration maneuver is not reliable, this information is not used in this step. Therefore, attitude angles, gyro misalignments, and gyro scale factor errors are estimated by EKF. The number of states in step 1 are reduced to 15, because the alignment of the star tracker is not considered. In step 2, 12 states related to the attitude angles, the gyro biases, and the two start tracker misalignments are estimated using all the measurements. Gyro alignment errors and scale factor errors estimated in step 1 are not estimated but just compensated in this step. In step 2, the payload measurements are accurate enough to identify the absolute alignments of the star trackers, because the spacecraft does not maneuver in this step. The convergence performance and the accuracy of the EKF are remarkably improved by the proposed method.

Since most equations related to the attitude dynamics and the filtering are well explained in [5,6], we mainly concentrate on the development of the proposed method in detail. In the following section, error models for a gyro and a star tracker are discussed. Then, the state and measurement equations used for the step 1 and the step 2 are represented. Numerical simulations are performed on a full scale spacecraft model to illustrate the performance of the proposed method. The conclusions are provided in the final section.

Sensor Models

Gyro misalignment and scale factor error model[6]

The measured gyro angular rate vector w_{gm} related to the true angular rate vector w_b is given by

$$\begin{aligned} w_{gm} &\equiv [\, w_x \; w_y \; w_z]^T \\ &= (I-\Lambda)(I-\Delta)\, T_b^g w_b - b_g - \eta_a \end{aligned} \tag{1}$$

where b_g is the gyro bias vector and η_a is the drift-rate white noise with covariance $E(\eta_a\eta_a^T)=\Sigma_a$. $\tilde{\Lambda}$ and $\tilde{\Delta}$ denote the scale factor error and the gyro alignment error, respectively. T_b^g represents the transformation matrix from the body frame to the gyro frame.

Assume that the gyro bias is given by the random walk model $db_g/dt=\eta_r$, where η_r is the random walk noise with covariance $E(\eta_r\eta_r^T)=\Sigma_r$. Using Eq. (1), the true angular rate is obtained as

$$\begin{aligned} w_b &= T_g^b(I-\tilde{\Delta})^{-1}(I-\tilde{\Lambda})^{-1}(w_{gm}+b_g+\eta_a) \\ &\approx T_g^b(I+\Delta)(I+\Lambda)(w_{gm}+b_g+\eta_a) \\ &= T_g^b(I+M)(w_{gm}+b_g+\eta_a) \end{aligned} \tag{2}$$

Note that $\Delta\simeq\tilde{\Delta}$, $\Lambda\simeq\tilde{\Lambda}$ and $M\simeq\Delta\Lambda$, because alignments errors and scale factor errors are very small. In Eq. (2), the term $I+\Delta$ is defined as the sum of orthogonal small angle rotation matrices along each axis.

Let $w'\equiv[\ w_x'\ \ w_y'\ \ w_z']^T=(I+\Lambda)(w_{gm}+b_g+\eta_a)$, then

$$\begin{aligned} (I+\Delta)(I+\Lambda)(w_{gm}+b_g+\eta_a) &= (I+\Delta)w' \\ &= \begin{bmatrix} 1 & -\delta_{xz} & \delta_{xy} \\ \delta_{xz} & 1 & 0 \\ -\delta_{xy} & 0 & 1 \end{bmatrix}\begin{bmatrix} w_x' \\ 0 \\ 0 \end{bmatrix} + \begin{bmatrix} 1 & -\delta_{yz} & 0 \\ \delta_{yz} & 1 & -\delta_{yx} \\ 0 & \delta_{yx} & 1 \end{bmatrix}\begin{bmatrix} 0 \\ w_y' \\ 0 \end{bmatrix} \\ &\quad + \begin{bmatrix} 1 & 0 & \delta_{zy} \\ 0 & 1 & -\delta_{zx} \\ -\delta_{zy} & \delta_{zx} & 1 \end{bmatrix}\begin{bmatrix} 0 \\ 0 \\ w_z' \end{bmatrix} \\ &= \begin{bmatrix} 1 & -\delta_{yz} & \delta_{zy} \\ \delta_{xz} & 1 & -\delta_{zx} \\ -\delta_{xy} & \delta_{yx} & 1 \end{bmatrix}\begin{bmatrix} w_x' \\ w_y' \\ w_z' \end{bmatrix} \end{aligned} \tag{3}$$

Neglecting the second order terms, we can write

$$\begin{aligned} I+M &= (I+\Delta)(I+\Lambda) \\ &\approx \begin{bmatrix} 1+\lambda_x & -(1+\lambda_y)\delta_{yz} & (1+\lambda_z)\delta_{zy} \\ (1+\lambda_x)\delta_{xz} & 1+\lambda_y & -(1+\lambda_z)\delta_{zx} \\ -(1+\lambda_x)\delta_{xy} & (1+\lambda_y)\delta_{yx} & 1+\lambda_z \end{bmatrix} \\ &= \begin{bmatrix} 1+\lambda_x & \bar{\delta}_{yz} & \bar{\delta}_{zy} \\ \bar{\delta}_{xz} & 1+\lambda_y & \bar{\delta}_{zx} \\ \bar{\delta}_{xy} & \bar{\delta}_{yx} & 1+\lambda_z \end{bmatrix} \end{aligned} \tag{4}$$

where

$$M=\begin{bmatrix} \lambda_x & \bar{\delta}_{yz} & \bar{\delta}_{zy} \\ \bar{\delta}_{xz} & \lambda_y & \bar{\delta}_{zx} \\ \bar{\delta}_{xy} & \bar{\delta}_{yx} & \lambda_z \end{bmatrix} \tag{5}$$

From Eq. (2) and Eq. (5), true angular rate vector can be rewritten as

$$w_b = T_g^b w_{gm} + T_g^b(I+M)b_g + T_g^b\Omega_g\delta_g + T_g^b(I+M)\eta_a \tag{6}$$

where Ω_g and δ_g are defined by

$$\Omega_g=\begin{bmatrix} w_{gm}{}^T & 0 & 0 \\ 0 & w_{gm}{}^T & 0 \\ 0 & 0 & w_{gm}{}^T \end{bmatrix} \tag{7}$$

$$\delta_g=[\ \lambda_x\ \ \bar{\delta}_{yz}\ \ \bar{\delta}_{zy}\ \ \bar{\delta}_{xz}\ \lambda_y\ \ \bar{\delta}_{zx}\ \ \bar{\delta}_{xy0}\ \ \bar{\delta}_{yx}\ \lambda_z]^T \tag{8}$$

Note that Ω_g is given as the rate gyro measurements and δ_g is the constant vector to be estimated.

Star tracker misalignment model

Quaternion operators are defined in the appendix. Let s, s_0, b, and eci denote the star tracker frame, the nominal frame, the body frame and the earth centered inertial frame. The quaternion observed in the star tracker coordinate is given by

$$q^s_{eci} = q^s_{s_0} \otimes q^{s_0}_b \otimes q^b_{eci} \tag{9}$$

where q^j_i denotes the quaternion from i-frame to j-frame, and the operator $\otimes$ is explained in the Appendix. Misalignment angle is small that $q^s_{s_0}$ can be approximated as

$$q^s_{s_0} \simeq \begin{bmatrix} \frac{1}{2}\delta_s \\ 1 \end{bmatrix} \tag{10}$$

where δ_s is a small angle rotation misalignment vector to be estimated. In this paper, two star trackers are used to determine the attitude of the spacecraft.

Alignment Calibration

Relative Gyro Calibration(Step 1)

In step 1, it is assumed that one of star trackers provides perfect information without any alignment error. In general, since the payload information yields very poor measurements during the calibration maneuver, we do not use this measurements to avoid the erroneous estimation of the alignments and scale factors of the gyro. Therefore, the estimated states are the alignments and scale factor errors of the gyros δ_g in addition to the vector part of the quaternion δq_v and the gyro bias error δb. Indeed, the estimated states in this step are corrupted by the alignment error of the star tracker, but they will be compensated in the next step by simple algebraic equations. Kinematics equations used in this step are defined by

$$\frac{d}{dt}\begin{bmatrix} \delta q_v \\ \delta b \\ \delta_g \end{bmatrix} = \begin{bmatrix} -[w^b\times] & 1/2T^b_g & 1/2T^b_g\Omega_g \\ 0 & 0 & 0 \\ 0 & 0 & 0 \end{bmatrix}\begin{bmatrix} \delta q_v \\ \delta b \\ \delta_g \end{bmatrix} + \begin{bmatrix} 1/2T^b_g(I+M) & 0 & 0 \\ 0 & I & 0 \\ 0 & 0 & I \end{bmatrix}\begin{bmatrix} \eta_a \\ \eta_r \\ \eta_g \end{bmatrix} \tag{11}$$

where r represents the nominal coordinate frame about the star tracker, η_a and η_g are the white noise included in δq_v and δ_g, respectively.
Measurement model is given by

$$z_k \equiv [I \ 0 \ 0]\begin{bmatrix} \delta q_v \\ \delta b \\ \delta_g \end{bmatrix} + \begin{bmatrix} \eta_s \\ 0 \\ 0 \end{bmatrix} \tag{12}$$

where $\hat{q}^*$ is the conjugate of the estimated quaternion z_k and η_s denote the vector part of $q^s_{eci} \otimes \hat{q}^*$ and the related white Gaussian noise, respectively.

Measurement equation given in Eq. (12) is linear, but the state equation given in Eq. (11) is nonlinear. Therefore, the Jacobian or sensitivity matrix of the state equation for EKF is required [6]. The states to be estimated can be reduced to 15 during the calibration maneuver, while 21 states should be estimated when the method in [6] is considered. The proposed method can estimate the alignment and the scale factors of the gyros more efficiently, although these states are biased by the misalignment of the star trackers. As mentioned earlier, they will be compensated in step 2. From Eq. (6), we can see that the gyro scale factor errors and alignment errors are not observable if the spacecraft is not rotating[6]. The sinusoidal calibration maneuver with different frequency along each axis is recommended to maximize the observability.

Star tracker alignment calibration(Step 2)

In Step 2, the alignment of two star trackers are calibrated using the payload data obtained from the camera and GCP, and the scale factors and alignments of the gyro obtained from Step 1 are compensated. Kinematic equation with the attitude error, the bias error of the gyro and the misalignments of the two star trackers is given by

$$\frac{d}{dt}\begin{bmatrix} \delta q_v \\ \delta b \\ \delta_{s1} \\ \delta_{s2} \end{bmatrix} = \begin{bmatrix} -[w^b \times] & 1/2T_g^b & 0 & 0 \\ 0 & 0 & 0 & 0 \\ 0 & 0 & 0 & 0 \\ 0 & 0 & 0 & 0 \end{bmatrix} \begin{bmatrix} \delta q_v \\ \delta b \\ \delta_{s1} \\ \delta_{s2} \end{bmatrix} + \begin{bmatrix} 1/2T_g^r(I+M) & 0 & 0 & 0 \\ 0 & I & 0 & 0 \\ 0 & 0 & I & 0 \\ 0 & 0 & 0 & I \end{bmatrix} \begin{bmatrix} \eta_a \\ \eta_r \\ \eta_{s1} \\ \eta_{s2} \end{bmatrix} \tag{13}$$

where δ_{s1} and δ_{s2} represent the misalignment of the star trackers with respect to body frame, respectively. Note that the scale factor errors and alignments errors of the gyro are not included in Eq. (13). Jacobian of the state equation for EKF is derived given in Ref. [6].
The measurement equation is given by

$$z = \begin{bmatrix} \vec{z}_{ks1} + \eta_{s1} \\ \vec{z}_{ks2} + \eta_{s2} \\ \vec{z}_{kp} + \eta_p \end{bmatrix} \tag{14}$$

where $\vec{z}_{ks1}$, $\vec{z}_{ks2}$ and $\vec{z}_{kp}$ are the vector part of the quaternion given by $q^{s1}_{eci} \otimes \widehat{q^{s1}_{eci}}^*$, $q^{s2}_{eci} \otimes \widehat{q^{s2}_{eci}}^*$, and $q^{b}_{eci}|_p \otimes \widehat{q}^*$ that denote the attitude errors to the star tracker 1, the star tracker 2 and the payload, respectively. η_{s1}, η_{s2} and η_p are the white Gaussian noises related to each measurement.

Now, let us investigate the measurement sensitivity matrix for EKF. The small perturbed measurement equation to q^b_{eci} using Eq. (9) is given by

$$\begin{aligned} \delta q^s_{eci} &= q^s_{eci} \otimes (q^s_b \otimes q_{r'})^* = (q^s_b \otimes \delta q \otimes q_{r'}) \otimes (q^s_b \otimes q_{r'})^* \\ &= q^s_b \otimes (q^{s*}_b * \delta q) = [q^s_b \otimes][q^{s*}_b *]\delta q = \begin{bmatrix} T^s_b & 0 \\ 0 & 1 \end{bmatrix} \delta q \end{aligned} \tag{15}$$

where the operator $*$ is defined in the appendix, and $q_{r'}$ denotes the perturbed body frame. On the other hand, the misalignment quaternion can be approximated by

$$\begin{aligned} \delta q^s_{eci} &= (q^s_{s0} \otimes q^{s0}_{eci}) \otimes q^{s0*}_{eci} = q^s_{s0} \\ &\approx \begin{bmatrix} 1/2\delta_s \\ 1 \end{bmatrix} \end{aligned} \tag{16}$$

Partial derivatives of Eq. (15) and Eq. (16) with respect to δq_v and δ_s, respectively, give

$$\begin{aligned} \frac{\partial \delta q^s_{eci,v}}{\partial \delta q_v} &= T^s_b \\ \frac{\partial \delta q^s_{eci,v}}{\partial \delta_s} &= \frac{1}{2} I \end{aligned} \tag{17}$$

Therefore, the sensitivity matrix of Eq. (14) becomes

$$H = \begin{bmatrix} T^{s1}_b & 0 & \frac{I}{2} & 0 \\ T^{s2}_b & 0 & 0 & \frac{I}{2} \\ I & 0 & 0 & 0 \end{bmatrix} \tag{18}$$

Since the number of states to be estimated in step 2 reduces to 12, the convergence characteristics is greatly improved compared with the AKF method in [6].

Gyro scale factors/misalignments compensation

Since the alignment error of the star tracker are neglected in step 1, the scale factor error and alignment error matrix M given in Eq. (5) must be compensated recursively using true alignment of the star trackers estimated in Step 2.

Let $\widetilde{M}$ denote the erroneous M represented by Eq. (5) due to the assumption of perfect star tracker alignment, then the erroneous estimates of body rate $\widetilde{w_b}$ using Eq. (2) is given by

$$\widetilde{w_b} = T_b^g(I+\widetilde{M})(w_{gm}+b_g+\eta_a) \tag{19}$$

Let $\tilde{b}$ denote the erroneous body frame, then $\widetilde{w_b}$ can also be calculated as

$$\widetilde{w_b} = T_b^{\tilde{b}} w_b \tag{20}$$

Substituting Eq. (23) into Eq. (5) and comparing with Eq. (21) to yield

$$T_b^{\tilde{b}} T_b^g(I+M) = T_b^g(I+\widetilde{M}) \tag{21}$$

or

$$M = T_g^b T_{\tilde{b}}^b T_b^g(I+\widetilde{M}) - I \tag{22}$$

where the transformation matrix from the true to the erroneous body frame $T_b^{\tilde{b}}$ is given by

$$T_b^{\tilde{b}} = T_{s0}^{\tilde{b}} T_b^{s0} \tag{23}$$

where $s0$ denotes the reference star tracker coordinate frame.
For small angle assumption of the misalignment of the star tracker, we have

$$T_{s0}^{\tilde{b}} \approx T_{s0}^b(I+\Delta_s) \tag{24}$$

where

$$(I+\Delta_s) = \begin{bmatrix} 1 & -\delta_{yz}^s & \delta_{zy}^s \\ \delta_{xz}^s & 1 & -\delta_{zx}^s \\ -\delta_{xy}^s & \delta_{yx}^s & 1 \end{bmatrix} \tag{25}$$

Hence, $T_b^{\tilde{b}}$ in Eq. (22) is calculated by

$$T_b^{\tilde{b}} = T_{s0}^b(I+\Delta_s)T_b^{s0} \tag{26}$$

In summary, true scale factor and alignment of the gyros are updated by Eq. (22) and Eq. (26). In this study, $\widetilde{M}$ is given in step 1 and the alignment error of the star tracker Δ_s is estimated in step 2. As the step 2 goes on, M converges to true value.

Simulation

For the performance test of the proposed method, the spacecraft assumed to be a earth observation satellites(EOS) locating on geo-synchronous orbit. The EOS has two star trackers, three fog gyros and a earth observing camera. The following error sources of the attitude sensors of the spacecraft are considered:

<u>Gyro</u>

- Random walk variance, drift stability : $0.005\deg/\sqrt{h}$, $0.05\deg/h$
- Scale factor $\lambda=(500,500,500)^T$ppm
- Misalignments $d_{xy}=200$, $d_{xz}=100$, $d_{yx}=300$, $d_{yz}=200$, $d_{zx}=400$, $d_{zy}=300$ arcsec

Star tracker
- Accuracy : 2 arcsec in non-rotating phase
- Misalignment : $\delta_{s1}=(20,20,20)^T$, $\delta_{s2}=(20,20,10)^T$ arcsec

Payload information
- Accuracy : 2 arcsec in non-rotating phase
- Update rate : 1sec

During the calibration maneuver, the spacecraft performs sinusoidal rotation with the magnitude of $0.5\deg/s$ and different frequencies of 0.0095, 0.008, 0.0085 *Hz* along each axis. After finishing calibration maneuver, we assume that the spacecraft rotates earth once per one day. The results obtained from step 1 and step 2 are shown in Figs. 1-6 and Figs. 7-14, respectively.

As shown in Fig. 1, the attitude estimation errors show sine curve due to the sinusoidal calibration maneuver. The gyro alignment estimation errors(Figs. 3-5) and the gyro scale factor estimation errors(Fig. 6) in the step 1 converge to a certain value within 400 seconds. Convergence rate can be improved by introducing other type of calibration maneuver. These steady-state errors in the step 1 are caused by the star trackers' misalignment which is not to be estimated. It is obtained that the attitude and gyro bias estimation are improved in the step 2 as shown in Figs. 7 and 8. During step 2, the gyro alignment errors and the gyro scale factor errors given in step 1 are greatly reduced in several seconds in the step 2 as shown in Figs. 9-12. These results reflect that the proposed update scheme given by Eq. (22). Estimation errors of both star trackers' misalignments as shown in Fig. 13 and 14 are bounded in 4 arcsec.

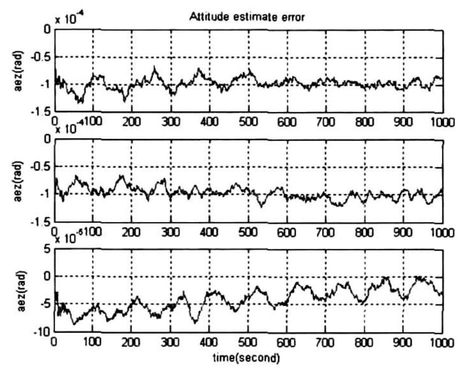

Fig. 1. Attitude estimation error(Step 1)

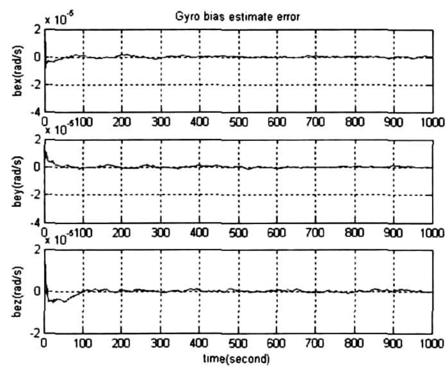

Fig. 2. Gyro bias estimation error(Step 1)

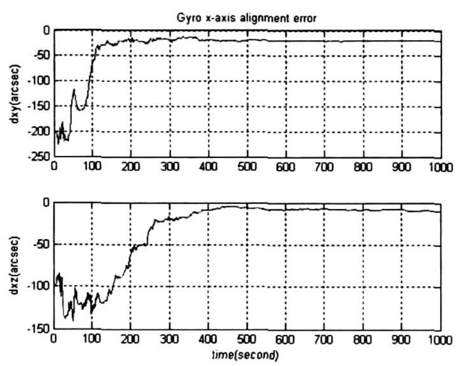

Fig. 3. Gyro x-axis alignment estimation error(Step 1)

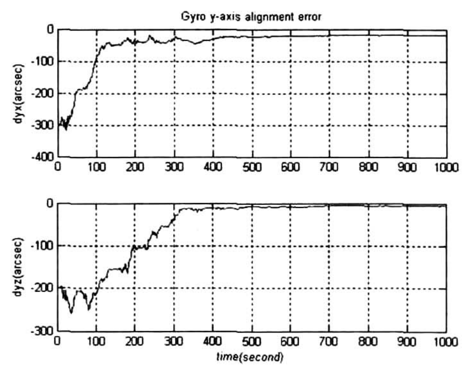

Fig. 4. Gyro y-axis alignment estimation error(Step 1)

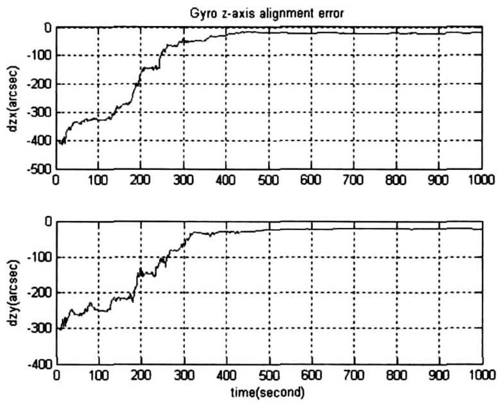

Fig. 5. Gyro z-axis alignment estimation error(Step 1)

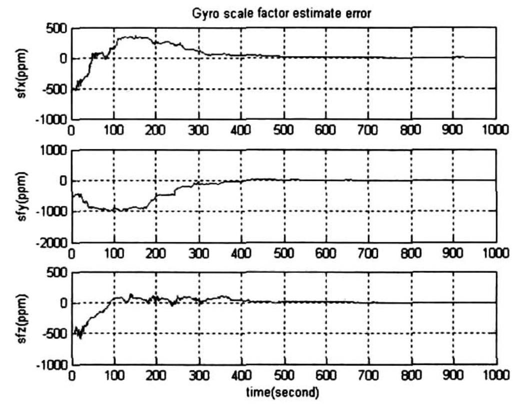

Fig. 6. Gyro scale factor estimation error(Step 1)

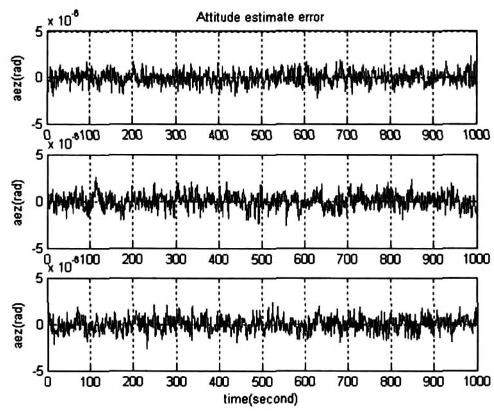

Fig. 7. Attitude estimation error (Step 2)

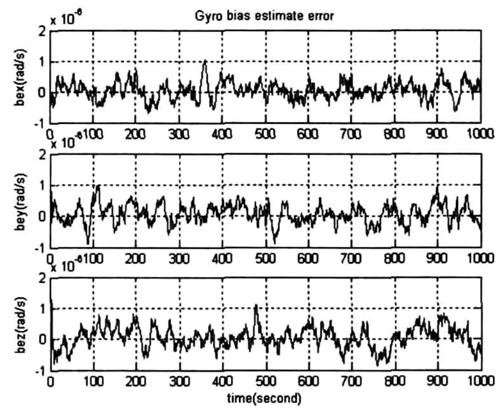

Fig. 8. Gyro bias estimation error (Step 2)

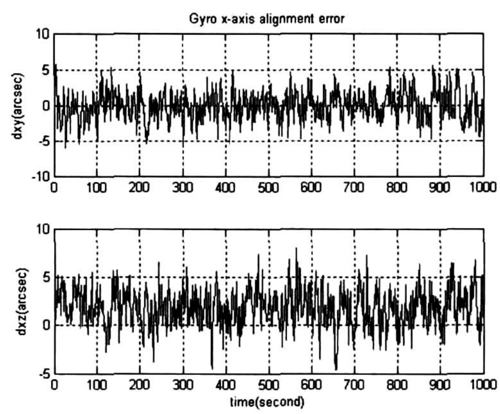

Fig. 9. Gyro x-axis alignment estimation error(Step 2)

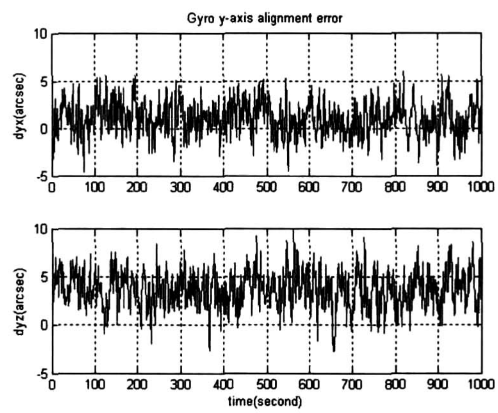

Fig. 10. Gyro y-axis alignment estimation error(Step 2)

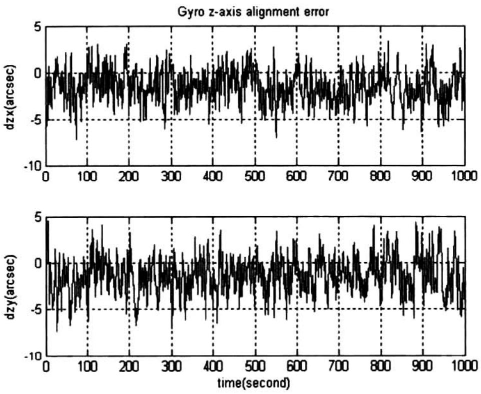

Fig. 11. Gyro z-axis alignment estimation error(Step 2)

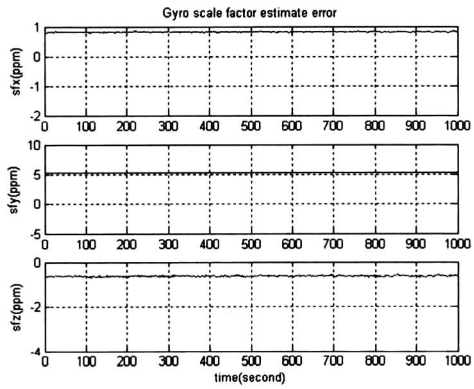

Fig. 12. Gyro scale factor estimation error(Step 2)

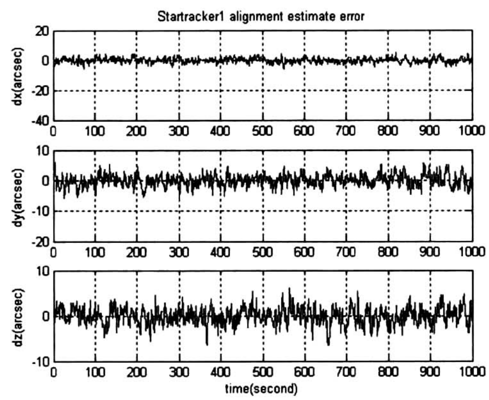

Fig. 13. Star tracker 1 alignment estimation error(Step 2)

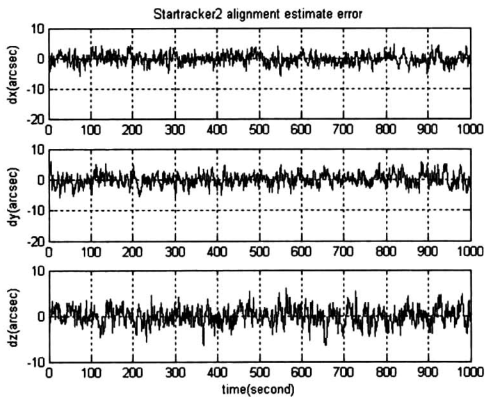

Fig. 14. Star tracker 2 alignment estimation error(Step 2)

The proposed method is compared with AKF. The computation time of AKF, step 1, and step 2 are appeared in Table. 2. Step 1 and step 2 of the proposed method reduces the computation time 31.5% and 15.8%, respectively.

Table 2. Computation time comparison(filter only)

Method		Computation time(ms)	Hardware specification
AKF		2.786	CPU: Pentium(R)-4 2.4GHz Memory: 512MB DDR ram O/S: MS Windows XP Program: Matlab ver.6.5
Proposed method	Step 1	1.9095	
	Step 2	2.3424	

The accuracy comparisons between AKF and the proposed method are shown in Table. 3. In AKF the sensor calibration s performed for 1000 seconds, while in the proposed method step 1 is performed for 800 seconds and then step 2 for 200 seconds. The accuracy of the payload measurement is assumed 10 arcsec during the calibration maneuver and 2 arcsec during pointing the earth on geo-synchronous orbit, respectively. Not shown in this paper, AKF shows bad accuracy for the calibration maneuver. Mean value and standard deviation of attitude estimation errors for 200 seconds after the calibration are shown in Table. 3. The proposed method are more accurate than AKF.

Table 3. Attitude estimation error comparisons

	Axis	Mean(arc-sec)	Standard deviation(arc-sec)
AKF	x-axis	-2.454	3.486
	y-axis	-0.466	3.361
	z-axis	-1.858	3.565
Proposed method	x-axis	-0.363	0.919
	y-axis	-0.098	1.639
	z-axis	-0.340	1.271

Conclusion

In this paper, we present an improved method for on-line calibration of gyros and star trackers for the precision spacecraft attitude determination by separating the gyro calibration process from the star tracker calibration process. Under the assumption of a perfect star tracker, the gyro calibration is performed to identify the scale factors and the alignments of the gyro during the calibration maneuver. Gyro calibration errors are then algebraically updated during the star tracker calibration process. In this process, camera and GCP information of the spacecraft are used to calibrate the absolute alignments of the star trackers. Extended Kalman filter is used for the estimation of the calibration parameters in both processes. The proposed method improves the performance and the implementation of the AKF. Simulation results show that the proposed method can determine the spacecraft attitude within the required precision.

Acknowledgement

This study was supported by National Research Lab.(NRL) Program(2002, M1-0203-00-0006) by the Ministry of Science and Technology, Korea. Authors fully appreciate the financial support. Also technical discussion with Dr. Jae-Cheol Yoon at Korea Aerospace Research Institute is highly acknowledged.

References

1. Friedland, B., "Treatment of Bias in Recursive Filtering," *IEEE Tr. on Automatic Control*, Vol. AC-14, No. 8, 1969, pp. 201-209.

2. Friedland B., "On the Calibration Problems," *IEEE Tr. on Automatic Control*, Vol. AC-22, No. 6, 1977, pp. 899-905.

3. Murrell, J. W., "Precision Attitude Determination for Multimission Spacecraft," *Proceedings of the AIAA Guidance and Control Conference*, New York, 1978, pp. 70-87.

4. Lefferts, E. J., Markley, F. L.,and Shuster, M. D., "Kalman Filtering for Spacecraft Attitude Estimation," *Journal of Guidance, Control, and Dynamics*, Vol. 5, No. 5, 1982, pp. 417-429.

5. Bae, S. and Bob, E. S., "Geoscience Laser Altimeter System (GLAS) Precision Attitude Determination," Algorithm Theoretical Basis Document, University of Texas at Austin, Oct., 2002.

6. Pittelkau, M. E., "Kalman Filtering for Spacecraft System Alignment Calibration," *Journal of Guidance, Control, and Dynamics*, Vol. 24, No. 6, November-December 2001, pp. 1187-1195.

7. Gelb, A, *Applied Optimal Estimation*, MIT Press, Cambridge, MA, 1989.

Appendix

Let p, q and r be quaternions and T_p, T_q and T_r be the corresponding transformation matrices. The operator $\otimes$ is defined by

$$r = p \otimes q = \begin{bmatrix} p_s & p_z & -p_y & p_x \\ -p_z & p_s & p_x & p_y \\ p_y & -p_x & p_s & p_z \\ -p_x & -p_y & -p_z & p_s \end{bmatrix} \begin{bmatrix} q_x \\ q_y \\ q_z \\ q_s \end{bmatrix} \tag{21}$$

The operator $*$ is defined by

$$r = q * p = \begin{bmatrix} q_s & -q_z & -q_y & q_x \\ q_z & q_s & -q_x & q_y \\ -q_y & q_x & q_s & q_z \\ -q_x & -q_y & -q_z & q_s \end{bmatrix} \begin{bmatrix} p_x \\ p_y \\ p_z \\ p_s \end{bmatrix} \tag{22}$$

Then $r = p \otimes q = q * p$ and corresponding transformation matrix is $T_r = T_p T_q$.
The conjugate is defined according to

$$p^* \otimes p = p \otimes p^* = \begin{bmatrix} 0 \\ 0 \\ 0 \\ 1 \end{bmatrix}$$

The following identities are used in this paper.

$$(p \otimes q)^* = q^* \otimes p^*$$

$$(q * p)^* = p^* * q^*$$

$$[q \otimes][q^* *] = \begin{bmatrix} T_q & 0 \\ 0 & 1 \end{bmatrix}$$

Where, $[q \otimes]$ and $[q *]$ represent the following operator matrices.

$$[q \otimes] = \begin{bmatrix} q_s & q_z & -q_y & q_x \\ -q_z & q_s & q_x & q_y \\ q_y & -q_x & q_s & q_z \\ -q_x & -q_y & -q_z & q_x \end{bmatrix}, \ [q *] = \begin{bmatrix} q_s & -q_z & -q_y & q_x \\ q_z & q_s & -q_x & q_y \\ -q_y & q_x & q_s & q_z \\ -q_x & -q_y & -q_z & q_s \end{bmatrix} \tag{25}$$